Journal of Comparative Physiology B
https://doi.org/10.1007/s00360-020-01286-1

ORIGINAL PAPER

Gills and air-breathing organ in O_2 uptake, CO_2 excretion, N-waste excretion, and ionoregulation in small and large pirarucu (*Arapaima gigas*)

Bernd Pelster[1,2] · Chris M. Wood[3,4] · Susana Braz-Mota[5] · Adalberto L. Val[5]

Received: 26 February 2020 / Revised: 15 May 2020 / Accepted: 29 May 2020

Abstract

In the pirarucu (*Arapaima gigas*), gill surface area and thus gas exchange capacity of the gills are reduced with proceeding development. It, therefore, is expected that *A. gigas*, starting as a water breather, progressively turns into an obligate air-breathing fish using an air-breathing organ (ABO) for gas exchange. We assessed the air-breathing activity, O_2 and CO_2 exchange into air and water, ammonia-N and urea-N excretion, ion flux rates, and activities of ion transport ATPases in large versus small pirarucu. We found that even very young *A. gigas* (4–6 g, 2–3 weeks post-hatch) with extensive gills are air-breathers (18.1 breaths*h^{-1}) and cover most (63%) of their O_2 requirements from the air whereas 600–700-g animals (about 3–4 months post-hatch), with reduced gills, obtain 75% of their O_2 from the air (10.8 breaths*h^{-1}). Accordingly, the reduction in gill surface area hardly affected O_2 uptake, but development had a significant effect on aerial CO_2 excretion, which was very low (3%) in small fish and increased to 12% in larger fish, yielding a hyper-allometric scaling coefficient (1.12) in contrast to 0.82–0.84 for aquatic and total CO_2 excretion. Mass-specific ammonia excretion decreased in approximate proportion to mass-specific O_2 consumption as the fish grew, but urea-N excretion dropped from 18% (at 4–6 g) to 8% (at 600–700 g) of total N-excretion; scaling coefficients for all these parameters were 0.70–0.80. Mass-specific sodium influx and efflux rates, as well as potassium net loss rates, departed from this pattern, being greater in larger fish; hyper-allometric scaling coefficients were > 1.0. Gill V-type H^+ ATPase activities were greater than Na^+, K^+-ATPase activities, but levels were generally low and comparable in large and small fish, and similar activities were detected in the ABO. *A. gigas* is a carnivorous fish throughout its lifecycle, and, despite fasting, protein oxidation accounted for the major portion (61–82%) of aerobic metabolism in both large and small animals. ABO PO_2 and PCO_2 (measured in 600–700-g fish) were quite variable, and aerial hypoxia resulted in lower ABO PO_2 values. Under normoxic conditions, a positive correlation between breath volume and ABP PO_2 was detected, and on average with a single breath more than 50% of the ABO volume was exchanged. ABO PCO_2 values were in the range of 1.95–3.89 kPa, close to previously recorded blood PCO_2 levels. Aerial hypoxia (PO_2 down to 12.65 kPa) did not increase either air-breathing frequency or breath volume.

Keywords Air-breathing fish · Gas exchange · Teleost · Ion regulation · Nitrogen excretion

Introduction

The teleost fish *Arapaima gigas* (Osteoglossidae), also named 'pirarucu' in the Brazilian Amazon, is one of many Amazonian fish that rely on air as a respiratory medium to support aerobic metabolism (Brauner and Val 1996; Gonzalez et al. 2010). Its respiratory and ionoregulatory physiology was first extensively studied on the Alpha Helix Expedition of 1976 (Bartlett 1980; Farrell and Randall 1978; Hochachka et al. 1978; Hulbert et al. 1978; Isaacks et al. 1977; Johansen et al. 1978; Randall et al. 1978; Stevens and Holeton 1978). It is generally believed that the

Communicated by G. Heldmaier.

Bernd Pelster and Chris M. Wood contributed equally to this paper.

✉ Chris M. Wood
woodcm@zoology.ubc.ca

Extended author information available on the last page of the article

Published online: 11 June 2020

frequently encountered hypoxic conditions in the Amazon basin (Diaz and Breitburg 2009; Muusze et al. 1998; Val and Almeida-Val 1995; Welker et al. 2013) are an important factor contributing to the evolution of air-breathing capacities in Amazonian fish (Bayley et al. 2018). According to Graham (1997), air-breathing evolved at least 68-times independently, while Damsgaard et al. (2019) concluded that air-breathing evolved 82 times from different water-breathing ancestors. Osteoglossid fish are basal teleosts; therefore, analysis of the aerial and aquatic gas exchange in the pirarucu may contribute to our understanding of the evolution of air-breathing in fish.

Due to the single circulatory loop of fish, oxygen taken up in the air-breathing organ (ABO) is returned to the heart. Leaving the ventricle, blood initially passes the gills, where in hypoxic water the oxygen may be lost to the water (Ishimatsu 2012). This has indeed been shown for air-breathing catfish (*Hypostomus aff. pyreneusi*), for example, or for the bowfin *Amia calva* and the spotted gar *Lepisosteus osseus* (Randall et al. 1981; Scott et al. 2017; Smatresk 1986; Smatresk and Cameron 1982). To reduce the possible oxygen loss at the gills, branchial surface area is often reduced in air-breathing fish, as shown for the erythrinid fish *Hoplias malabaricus* and *Hoplerythrinus unitaeniatus* (Cameron and Wood 1978; Pelster et al. 2018). As reviewed by Pelster and Wood (2018), the reduction of the surface area of the gills has implications for a number of physiological phenomena including ion homeostasis and N-waste excretion (Wood et al. 2016), oxidative stress management (Pelster et al. 2016, 2018) as well as water regulation and acid–base homeostasis (Bayley et al. 2018; Brauner et al. 2004; Shartau and Brauner 2014).

In *Arapaima*, the progressive reduction of gill surface area can be observed with development. After hatching, the gill filaments bear typical gill lamellae, the site of aquatic gas exchange. In a 10-g fish, about 4 weeks after hatching, these lamellae are clearly visible (Brauner et al. 2004). With further development, these lamellae disappear, so that in a 100-g fish, some rudimentary lamellae are found, and in a 1-kg fish, they are completely gone (Brauner et al. 2004; Ramos et al. 2013). The water-to-blood diffusion distance also increases greatly. Based on these observations, it is generally believed that the pirarucu initially is a water breather (Graham 1997) and then with proceeding development switches to a breathing air, and finally becomes an obligatory air-breathing fish that drowns if access to air is denied (Brauner et al. 2004). Gonzalez et al. (2010) reported that fish of about 60–70 g take up about 76% of O_2 from the air, while CO_2 (86%) is primarily excreted to the water. Curiously in tenfold larger fish (~ 700 g), these same authors reported that the fraction of O_2 uptake from the air was actually smaller (70%) and the fraction of CO_2 excretion to the water was actually greater (89%). While these differences were small, they were statistically significant. In 2000–3000-g pirarucu, 78% of O_2 uptake was from air (Stevens and Holeton 1978) and 63% of CO_2 excretion was to the water (Randall et al. 1978). Overall, these data suggest that quantitative evidence for the developmental transition in respiratory function must be sought in pirarucu much smaller than 70 g. Nevertheless, the concept of a switch in gas exchange from a water-breather to an air-breather with development is supported by observations of longer survival times of small fish (10 g versus 1 kg) when access to air was denied (Brauner et al. 2004). It is also supported by the finding that pirarucu in the early developmental stages use ATP and GTP as organic phosphates in the blood to modify hemoglobin oxygen affinity and thus hemoglobin oxygen transport, but with proceeding development switch to inositol pentaphosphate (IPP) as the main erythrocytic organic phosphate (Isaacks et al. 1977; Val et al. 1992). IPP is typically found in birds and reptiles, for example, and usually is more effective in the reduction of hemoglobin oxygen affinity than ATP or GTP (Bartlett 1980). In air, the oxygen capacity is—depending on the temperature—20 to 30 times higher than in water, and hemoglobin oxygen affinity in air-breathers has been shown to be lower than in water breathers (Bayley et al. 2018; Johansen et al. 1978).

The comparison of 70-g versus 700-g pirarucu by Gonzalez et al. (2010) also raises some interesting questions about developmental changes in ion exchange and N-waste excretion. Surprisingly, despite the reduced gill surface area in larger fish, the mass-specific unidirectional Na^+ influx (J_{in}^{Na+}) and passive Na^+ efflux (J_{out}^{Na+}) rates were both about threefold higher than in small fish, and this occurred despite lower specific activity of Na^+, K^+-ATPase (NKA) in the gills of the larger fish. Total mass-specific ammonia and urea-N excretion rates were both only about 1.6-fold higher, in contrast to the 2.75-fold higher total mass-specific MO_2 (total MCO_2 was not reported) in these same small fish. This would suggest either that very different allometric scaling must occur for these various gill-dependent processes, or that the fish compared by Gonzalez et al. (2010) were in very different physiological conditions.

With this background in mind, in the present study, we examined much smaller pirarucu and compared their physiology with 600–700 g animals, very similar in size to the large (~ 700 g) pirarucu used by Gonzalez et al. (2010). Contingent upon availability, we used small fish of approximately 5 g (2–3 weeks post-hatch) for respiratory gas exchange and N-waste excretion measurements, and 20-g fish (6–7 weeks post-hatch) for determinations of unidirectional Na^+ flux rates, net ion balance, N-waste excretion rates (again), and branchial NKA and vH^+ ATPase activities. Large fish of 600–700 g (3–4 months post-hatch) were used for all comparative measurements. All fish were fasted for 2–3 days. We hypothesized that these very early

developmental stages with well-developed gill lamellae would rely to a much greater extent on water-breathing. We also hypothesized that in comparison to the large fish, they would demonstrate much higher mass-specific rates for all processes (MO_2, MCO_2, M_{Amm}, $M_{Urea\text{-}N}$, J_{in}^{Na+}, J_{out}^{Na+}) with greater fractional dependence on the gills versus ABO for both MO_2 and MCO_2. We further hypothesized that scaling coefficients would be fairly uniform for those processes depending mainly on gill function.

By simultaneous measurements of MO_2 and MCO_2 in the water and air phases, the importance of the ABO versus the gills for both processes was analyzed in small and large pirarucu. To measure MCO_2, we employed novel optical PCO_2 micro-sensors (Lee et al. 2018; Wood and Eom 2019). Together with optical PO_2 micro-sensors, these also allowed us to assess the functioning of the ABO under aerial normoxia and hypoxia, with measurements of breathing frequency, breath volume, ABO gas composition, and respiratory gas exchange ratios. Based on preliminary observations of Farrell and Randall (1978) who manipulated the gas composition of the ABO, we hypothesized that aerial hypoxia would increase air-breathing frequency and breath volume.

Materials and methods

Experiments were performed at the Laboratory of Ecophysiology and Molecular Evolution (LEEM) of the Brazilian National Institute for Research of the Amazon (INPA) in Manaus, Brazil. All experimental protocols were in compliance with INPA animal care regulations. *Arapaima gigas* of several different sizes were obtained from a commercial fish culture in Manaus, brought to the LEEM/INPA and kept in outdoor fish tanks, supplied with running INPA well water. The water was continuously aerated and fish had free access to air. Fish were fed daily with commercial pellets (NutripeixeTr36, Purina Co., São Paulo, SP, Brazil 36% protein) of the appropriate size but fasted for 2–3 days before the experiments. The composition of the water was $[Na^+] = 200–250$, $[K^+] = 10–20$, $[Ca^{2+}] = 3–5$, $[Mg^{2+}] = 3–8$, $[Cl^-] = 150–200$ µmol L^{-1}, pH 6.0–6.5. The acclimation and experimental temperature were 27–29 °C. In all experiments, animals were transferred to their individual experimental chambers and allowed to settle for several hours. The water was changed by siphon, without air-exposure of the animal, and then measurements commenced. The chambers were shielded in black plastic and continuously aerated prior to experiments.

Series 1

This series focused on O_2 and CO_2 exchange and included measurements of ammonia-N and urea-N excretion. Body mass of small *Arapaima* was 4.70 ± 0.38 g, fork length 10.4 ± 0.1 cm (2–3 weeks post-hatch; $N = 16$). Body mass of large *A. gigas* was 625 ± 48 g, fork length 47.1 ± 0.7 cm (3–4 months post-hatch; $N = 15$). These large fish also furnished the tissue samples of Series 3.

Respirometry and N-waste excretion measurements in large versus small pirarucu

O_2 uptake (MO_2) and CO_2 excretion (MCO_2) were determined by closed respirometry, using two chambered respirometers similar to those of Stevens and Holeton (1978). In these experiments, aeration was stopped and the respirometers were sealed for 0.5–1.1 h so that water PO_2 did not drop below 80% of aerial PO_2. For large pirarucu, the volume of the water compartment was 7.7 l or 7.95 l, with an air chamber of 320 ml or 321 ml, respectively. The volume of the water chamber for small pirarucu was 502 ml, with an air chamber of 12.4 ml. Oxygen partial pressure in water was determined using a portable oxygen meter (WTW Multi3410 meter, Weilheim, Germany). PCO_2 levels in water and in air were measured using PreSens PCO_2 profiling micro-sensors provided as prototypes by PreSens Precision Sensing GmbH (Regensburg, Germany). The PCO_2 optodes were calibrated before each experiment using water samples equilibrated with defined PCO_2 levels provided by a gas-mixing pump (SA27/2, Wösthoff Messtechnik GmbH, Bochum, Germany). While these optodes were originally designed to measure PCO_2 levels only in fluids, we found that they functioned well and maintained calibration in the humid gas phase (90–100% relative humidity) of the ABO and the air spaces of our respirometers. PO_2 in the air was determined using PreSens fiber optic oxygen sensors, calibrated with aerial oxygen and pure nitrogen. Both PCO_2 and PO_2 microsensors were protected inside 23-guage hypodermic needles; the fluorophore tips were advanced out of the needles into air or water phases to make measurements. The top of the air chamber was closed with a rubber bung. For continuous recording of air PO_2 and PCO_2, the two PreSens optodes were poked through the rubber bung.

In a two-chambered respirometer with air and water chambers, oxygen may diffuse from the air into the water, resulting in an underestimation of aquatic oxygen uptake. We tested the stability of aquatic PO_2 (PO_2 about 13 kPa) with a normoxic PO_2 of 20 kPa in the air chamber. Water PO_2 was stable for more than 1 h. However, when the fish is present, it periodically breaks the surface, and this may increase diffusive exchange. Stevens and Holeton (1978)

with a similar set-up estimated that the error in MO_2 from either phase would be below 10%.

Mass-specific oxygen consumption in water (MO_{2water}) was calculated as

$$\mathrm{MO}_{2\,\mathrm{water}} = a\mathrm{O}_2 \times \Delta P_\mathrm{w}\mathrm{O}_2 \times V_\mathrm{w} \times T^{-1} \times \mathrm{BM}^{-1}, \quad (1)$$

where αO_2 is the physical solubility of oxygen in water at the experimental temperature (Boutilier et al. 1984), ΔP_wO_2 is the change in O_2 partial pressure in the water, V_w is the water volume of the respirometer chamber, T represents the time of closing the respirometer, and BM is body mass. Similarly, aquatic CO_2 excretion was determined using the change in CO_2 partial pressure (ΔP_wCO_2) and the solubility of CO_2 (αCO_2) in the experimental water. The latter was determined by equilibrating INPA water with 100% CO_2 and then measuring its total CO_2 content with a Corning 965 Analyser (Ciba-Corning, Halstead, Essex, UK). The resulting αCO_2 value (0.03860 mmol L^{-1} $torr^{-1}$) agreed closely with the value (0.04129 mmol L^{-1} $torr^{-1}$) tabulated by Boutilier et al. (1984) for distilled water at 28 °C. CO_2 excretion into water is four- to sevenfold greater than ammonia excretion and clamps the water pH at circumneutrality. Therefore, in the presence of excess CO_2, all ammonia excreted into water of pH 6.0–6.5 (i.e. more than 2 log units below the pK of ammonia), acts as a base converting CO_2 to HCO_3^- in an equimolar fashion to form dissolved NH_4HCO_3. Thus, the portion of CO_2 converted to HCO_3^- due to the excretion of ammonia no longer contributes to the partial pressure of CO_2. Therefore, we corrected the water CO_2 excretion rates by adding the simultaneously measured values for ammonia excretion in that same fish:

$$\mathrm{MCO}_{2\mathrm{water}} = \alpha\mathrm{CO}_2 \times \Delta P_\mathrm{w}\mathrm{CO}_2 \times V_\mathrm{w} \times T^{-1} \times \mathrm{BM}^{-1} + M_{\mathrm{ammonia}}. \quad (2)$$

The rates of ammonia-N and urea-N excretion were calculated as

$$M_{\mathrm{amm}-N;\mathrm{urea}-N} = \left(C_\mathrm{F} - C_\mathrm{I}\right) \times V_\mathrm{w} \times T^{-1} \times \mathrm{BM}^{-1}, \quad (3)$$

where C_F and C_I are the final and initial concentrations of ammonia-N or urea-N in water and the other symbols are as above.

Aerial O_2 exchange was calculated as

$$\mathrm{MO}_{2\mathrm{air}} = b\mathrm{O}_2 \times \Delta P_\mathrm{a}\mathrm{O}_2 \times V_\mathrm{a} \times T^{-1} \times \mathrm{BM}^{-1} \quad (4)$$

and an entirely analogous equation was used for aerial CO_2 exchange:

$$\mathrm{MCO}_{2\mathrm{air}} = \beta\mathrm{CO}_2 \times \Delta P_\mathrm{a}\mathrm{CO}_2 \times V_\mathrm{a} \times T^{-1} \times \mathrm{BM}^{-1}, \quad (5)$$

where ΔP_aO_2 and ΔP_aCO_2 were the measured changes in respective partial pressures in the air phase, values for βO_2 and βCO_2 were taken from Dejours (1981), V_a is the volume of the air phase, and the other symbols are as above.

RQ values were calculated as

$$\mathrm{RQ} = \mathrm{MCO}_2 \times \mathrm{MO}_2^{-1} \quad (6)$$

separately for aerial and aquatic gas exchange and also for total gas exchange.

Nitrogen quotient (NQ) values were calculated as

$$\mathrm{NQ} = M_{\mathrm{total}-\mathrm{N}} \times \mathrm{MO}_2^{-1}, \quad (7)$$

where $M_{total\text{-}N}$ represents total urea-N ($M_{urea\text{-}N}$) + ammonia-N ($M_{amm\text{-}N}$) excretion.

Measurement of gas composition in the air-breathing organ of large pirarucu

A sphincter muscle in the first section of the esophagus connects the esophagus dorsally with the ABO. Under light anesthesia (Farrell and Randall 1978), a PE50 tubing (Becton, Dickinson and Co., Franklin Lakes, NJ, USA) was inserted into the ABO through this sphincter. The tubing was sutured securely to the inside of the mouth and guided through the upper lip via a short piece of heat-flared PE 160 tubing. Fish were returned to the respirometer chamber and left for recovery for at least 2 h. During the experiment, gas samples were collected from the ABO at various times after an air breath using a gas-tight glass syringe connected to the catheter tubing via a three-way stopcock. Prior to collecting a gas sample, the dead-space of the catheter was emptied into an additional syringe. The syringe with the gas sample (approximately 0.5 ml) was closed with a thick layer of parafilm and the PreSens micro-optodes were immediately inserted through the parafilm closure to measure PO_2 and PCO_2 in the gas sample. After the measurement, which typically was completed within 90 s, the gas sample was returned to the ABO to minimally disturb the air-breathing behavior.

Gas composition of the ABO was recorded together with aerial gas exchange. In *Arapaima*, exhalation occurs prior to inhalation, followed by an inspiration, and the whole process is completed within milliseconds (Farrell and Randall 1978). Accordingly, the volume of the exhaled air transiently increases the volume of the air chamber and modifies the PO_2 in the air chamber in proportion to the PO_2 in the exhaled air. Taking the transient increase of the air chamber volume by the exhaled breath into account, exhaled breath volume (V_b) can be calculated from the change in PO_2 in the air chamber of known volume (V_a) by addition of a breath of ABO air, where P_1 and P_2 are the initial (pre-exhalation) and final (post-exhalation) PO_2 values, respectively, and from P_{ABO}, representing the PO_2 in the ABO at the time of air breathing:

$$V_b \times P_{ABO} + V_a \times P_1 = (V_b + V_a) \times P_2, \quad (8)$$

PO_2 in the ABO at the time of air breathing was calculated from measured PO_2 values in the ABO extrapolated to the time of taking the next air breath, based on the recorded changes in ABO PO_2 following an air breath. Solving Eq. 8 for V_b results in

$$V_b = (V_a \times P_2 - V_a \times P_1)/(P_{ABO} - P_2). \quad (9)$$

Series 2

Ionic exchange and N-waste excretion in large versus small pirarucu

This series focused on ion exchange and again included measurements of ammonia-N and urea-N excretion. Body mass of small *Arapaima* was 20.45 ± 0.43 g (N = 28). These small fish also furnished the tissue samples of Series 3. Body mass of large *A. gigas* was 619 ± 54 g, fork length 47.5 ± 0.9 cm (N = 6). For large pirarucu, the same respirometer chambers were used as in Series 1, but the volume of the water phase was reduced to approximately 4 L (exact volume measured in each experiment) by the addition of plastic-wrapped bricks, to increase resolution in flux measurements. For small pirarucu, 1-L Erlenmeyer flasks were used with the initial water volume set to 0.745 L. Aeration was maintained throughout flux measurements to ensure mixing.

Unidirectional flux rates (J_{in}^{Na+}, J_{out}^{Na+}) and net flux rates (J_{net}^{Na+}) of sodium, as well as net flux rates of ammonia-N, urea-N, chloride, and potassium were measured over 3-h periods, as described by Wood (1992). Radioactive ^{22}Na (as NaCl, New England Nuclear Dupont, Boston, MA, USA, supplied by REM, Sao Paulo, SP, Brazil) was added (1 µCi = 37 kBq for small fish, 4 µCi = 148 kBq for large fish), allowed to mix for 15 min, and then water samples were taken at 0 h and 3 h for measurements of radioactivity (2 × 5 mL) and ion plus N-waste concentrations (20 mL). Net flux rates in µmol kg^{-1} h^{-1} of Na^+ (J_{net}^{Na+}), Cl^- (J_{net}^{Cl-}), and K^+ (J_{net}^{K+}) were calculated from changes in water concentrations (in µmol L^{-1}), factored by the known body mass (in kg), water volume (in L), and experimental time (in h), as in Eq. 3. By convention, ion fluxes out of the fish are negative, while fluxes into the fish are positive. The disappearance of radioactivity from the water (into the fish) yielded the Na^+ influx rate (positive):

$$J_{in}^{Na+} = \frac{([CPM_i] - [CPM_F]) \times V_w}{(SA_{ext} \times T \times BM)}, \quad (10)$$

where CPM_i initial radioactivity in the water (in cpm L^{-1}) at the start of the flux period, CPM_F final radioactivity in the water (in cpm L^{-1}) at the end of the flux period, SA_{ext} mean external specific activity (radioactivity per total Na^+) in the water (in cpm µmol^{-1}), calculated from measurements of water radioactivity and total water [Na^+] at the start and end of the flux period, and V_w (in L), T (in h), and BM (in kg) were as defined earlier.

J_{out}^{Na+} (negative) was calculated by difference:

$$J_{out}^{Na+} = J_{net}^{Na+} - J_{in}^{Na+}. \quad (11)$$

Series 3

Branchial and ABO enzyme activities in large versus small pirarucu

This series focused on measurements of Na^+, K^+-ATPase (NKA) and V-type H^+ ATPase (vH^+ ATPase) activities of gills and ABO. Large pirarucu (from Series 1) and small pirarucu (from Series 2) maintained under normoxic conditions were rapidly anesthetized with an overdose of tricaine methanesulfonate (MS222; 0.5 g L^{-1}) and killed by a sharp blow on the head. Fish were opened ventrally and the ABO was exposed. Samples of ABO tissue were rapidly dissected on both sides of the vertebra avoiding contact to the centrally positioned kidney and contamination of ABO tissue. Tissue samples were carefully rinsed, cleaned and blotted dry. In addition, gill tissue was rapidly dissected, cleaned and blotted dry. Tissue samples were immediately frozen in liquid nitrogen and then stored in a biofreezer at − 80 °C until further analysis.

Analytical techniques

Ammonia concentrations and urea-N concentrations in water were measured by the colorimetric methods (Rahmatullah and Boyde 1980; Verdouw et al. 1978). Radioactivity of ^{22}Na in water samples was measured by mixing 5 mL of water with 10 mL of Ultima Gold scintillation fluid (Perkin-Elmer, Waltham, MA, USA), and then counted on a Triathler portable counter (Hidex, Helsinki, Finland). Tests showed that quench was constant so correction was unnecessary. Water total Na^+ and K^+ concentrations were measured using a 910 Digital Flame Photometer (Instrumentação Analítica São Paulo, SP, Brazil), and water Cl^- concentrations by the colorimetric method of Zall et al. (1956).

Na^+, K^+ ATPase (NKA) and V-type H^+ ATPase were measured according to Kültz and Somero (1995), as previously described in detail (Wood et al. 2016). Note that there are concerns that NEM may not be specific (Forgac 1989), but Nawata et al. (2007) directly tested NEM against 10 µM bafilomycin and found the same results with the two inhibitors. Protein concentration in the homogenate was measured

with Coomassie Brilliant Blue G-250 (Bradford 1976) using bovine serum albumin as a standard.

Statistics

Data have been expressed as mean ± 1 SEM with N giving the number of animals analyzed. Enzyme activities are given as U mg^{-1} protein (μmol h^{-1} mg^{-1}protein). For enzyme activities, a two-way ANOVA with Holm–Sidak multiple comparison procedures was used, using body mass as parameter 1, tissue as parameter 2 and activity as a variable. Student's two-tailed *t* tests were used for comparison of gas exchange parameters, fractional gas exchange and RQ values between small and large *A. gigas*. Pearson correlation was used to test for a significant correlation between parameters. Scaling exponents for rate functions MO_{2water}, MO_{2air}, MO_{2total}, MCO_{2water}, MCO_{2air}, MCO_{2total}, $M_{amm\text{-}N}$, $M_{urea\text{-}N}$, $M_{total\text{-}N}$, $J^{Na+}{}_{in}$, and $J^{Na+}{}_{out}$ were calculated as the slopes of linear regressions of the log of individual rates (*Y*) against the log of body mass (*X*). Note that for $J_{net}{}^{Na+}$, $J_{net}{}^{K+}$, and $J_{net}{}^{Cl-}$, these calculations could only be done on size-group means, as these comprised data with both positive and negative values. The statistical analysis was performed using SigmaPlot 14.0. Statistical differences between values were accepted for $p < 0.05$.

Results

Series 1

Respirometry and N-waste excretion measurements in large versus small pirarucu

Aerial respiration of large *A. gigas* (600–700 g) in the two-chambered respirometer with each breath caused a stepwise decline in air-chamber PO_2, while the PCO_2 increased stepwise (Fig. 1a). Due to the longer response time of the CO_2 sensor, it took between 1 and 2 min, before the CO_2 signal was stable, while the O_2 sensor showed an instantaneous response. For small *A. gigas* (4–6 g) similar results were obtained (Fig. 1b), but due to the higher air-breathing frequency, the stepwise increase in PCO_2 was obscured. While large fish took an air breath every 5.58 ± 0.45 min (10.8 breaths*h^{-1}) at aerial PO_2 values above 18 kPa, small fish took a breath every 3.31 ± 0.19 min (18.1 breaths*h^{-1}, $p < 0.001$). Nevertheless, a clear increase in PCO_2 combined with a decrease in PO_2 was detected, demonstrating that even small *A. gigas* of about 5 g body mass breathe air.

Quantification of gas exchange for small and large *A. gigas* (Table 1) revealed that the mass-specific MO_{2total} of small fish from both air and water (11.18 ± 0.53 mmol kg^{-1} h^{-1}) was more than threefold higher than that of large fish (only 3.66 ± 0.40 mmol kg^{-1} h^{-1}). In large fish, the fraction of aerial MO_{2air} (75%) was significantly higher than in small fish (63%; Table 1). Overall mass-specific MCO_{2total} was also significantly higher in small fish by about 2.2-fold, but aerial MCO_{2air} contributed only 3% to the total CO_2 excretion, while large fish excreted 12% of the CO_2 into the air chamber (Table 1). Accordingly, the respiratory ratio (RQ) for aerial gas exchange was more than three times higher in larger fish. The respiratory ratio in water was almost twice as high in large animals as compared to the small fish. Overall the respiratory ratio was higher in larger fish (0.91 versus 0.72), but this difference was not significant (Table 1).

Like MO_2, mass-specific $M_{amm\text{-}N}$ in small *A. gigas* was more than threefold higher than in large individuals (1.94 ± 0.15 versus 0.57 ± 0.06 mmol-N kg^{-1} h^{-1}), whereas mass-specific $M_{urea\text{-}N}$ was almost tenfold higher in the 5-g fish (0.47 ± 0.06 versus 0.05 ± 0.01 mmol-N kg^{-1} h^{-1})

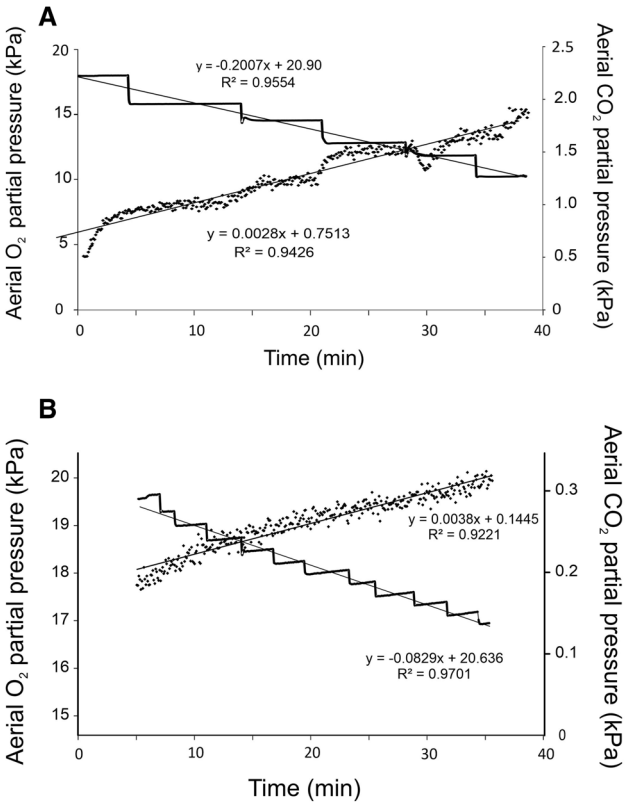

Fig. 1 Original recording of O_2 and CO_2 partial pressure in the air chamber of the respirometer in a large *A. gigas* (**a**), body mass 710 g; and in a small *A. gigas* (**b**), body mass 5.89 g, in Series 1. Air in the respiratory chamber was not renewed in this experiment and sequential breaths resulted in a stepwise decrease in aerial O_2 partial pressure and increase in CO_2 partial pressure. The less distinct steps for CO_2 in **a** and absence of steps for CO_2 in **b** reflects the slower response time of the PCO_2 sensor. Regression lines and R^2 values are shown, all highly significant ($p < 0.001$)

Table 1 A comparison of mass-specific rates of O_2 consumption (MO_2) and CO_2 excretion (MCO_2), fractional contributions of aerial respiration to total respiration, the respiratory exchange ratio (respiratory quotient) ($RQ = MCO_2/MO_2$), mass-specific rates of ammonia-N excretion ($M_{amm\text{-}N}$) and urea-N excretion ($M_{urea\text{-}N}$), fractional contribution of urea-N to total-N excretion, and nitrogen quotient ($NQ = M_{total\text{-}N}/MO_2$) of small and large *A. gigas* of Series 1

	Small *A. gigas*	Large *A. gigas*
Body mass (g)	4.7 ± 0.38 g (6)	687 ± 52[a] (10)
MO_{2air} (mmol kg^{-1} h^{-1})	7.09 ± 0.46 (6)	2.79 ± 0.73[a] (9)
MO_{2water} (mmol kg^{-1} h^{-1})	4.09 ± 0.37 (6)	0.91 ± 0.06[a] (10)
MO_{2total} (mmol kg^{-1} h^{-1})	11.18 ± 0.53 (6)	3.66 ± 0.40[a] (9)
MCO_{2air} (mmol kg^{-1} h^{-1})	0.24 ± 0.04 (6)	0.45 ± 0.07[a] (9)
MCO_{2water} (mmol kg^{-1} h^{-1})	7.75 ± 0.76 (6)	3.21 ± 0.31[a] (9)
MCO_{2total} (mmol kg^{-1} h^{-1})	7.99 ± 0.77 (6)	3.66 ± 0.36[a] (9)
Fraction aerial MO_2	0.63 ± 0.03 (6)	0.75 ± 0.02[a] (9)
Fraction aerial MCO_2	0.03 ± 0.001 (6)	0.12 ± 0.01[a] (9)
RQ air	0.07 ± 0.01 (6)	0.23 ± 0.08[a] (9)
RQ water	1.93 ± 0.18 (6)	3.49 ± 0.25[a] (9)
RQ	0.72 ± 0.06 (6)	0.91 ± 0.10 (9)
$M_{amm\text{-}N}$ (µmol-N kg^{-1} h^{-1})	1941.4 ± 154.3 (6)	565.7 ± 55.6[a] (10)
$M_{urea\text{-}N}$ (µmol-N kg^{-1} h^{-1})	466.9 ± 64.3 (6)	48.1 ± 7.8[a] (10)
$M_{total\text{-}N}$ (µmol-N kg^{-1} h^{-1})	2408.3 ± 197.3 (6)	613.8 ± 59.8[a] (10)
Fraction Urea-N	0.19 ± 0.02 (6)	0.08 ± 0.01[a] (10)
NQ	0.22 ± 0.03 (6)	0.16 ± 0.03 (10)

Means ± SEM (N)

[a]Significant differences between small and large fish

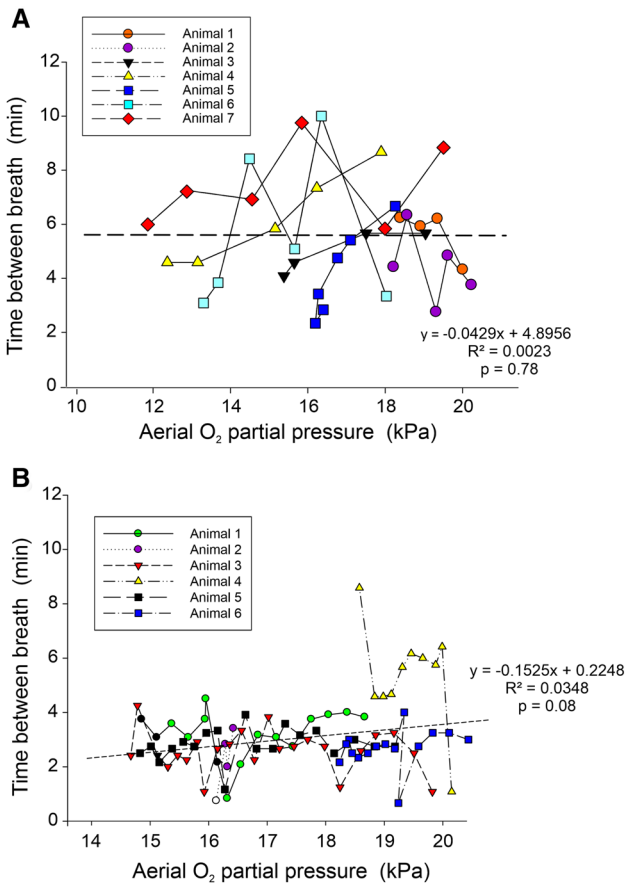

Fig. 2 The time between subsequent air-breaths with progressive aerial hypoxia in individual large (**a**) and small (**b**) *A. gigas*, in Series 1. Regression lines are shown; slopes are not significantly different from zero

(Table 1). As a result, their fraction of total-N waste excreted as urea-N (19%) was more than twice as high as in the large fish (8%). The overall NQ in small fish was 0.22, not significantly higher than 0.16 in the large animals (Table 1).

By breathing air, the fish slowly reduced the oxygen partial pressure in the air space. Plotting the time between subsequent air-breaths versus the PO_2 in the air space of the respirometer for large (Fig. 2a) as well as for small *A. gigas* (Fig. 2b) revealed that aerial hypoxia down to PO_2 values of 12.7–14.6 kPa of oxygen did not stimulate air-breathing; there was no increase in air-breathing frequency (Fig. 2).

The gas composition in the air-breathing organ of large pirarucu and the response to aerial hypoxia

To analyze the composition of gas in the ABO of large pirarucu, a gas sample was taken at varied times after an air-breath and the composition measured as shown in Fig. 3. Each air-breath caused a typical stepwise reduction in air space PO_2, because the exhaled breath diluted the PO_2. Figure 3a shows measurements taken under normoxic conditions, where a drop of aerial O_2 concentration below 18 kPa was avoided by renewing the airspace (flushing) during measurement of ABO PO_2. By transferring the O_2 and the CO_2 sensors from the respirometer air-space to the ABO gas sample, the actual ABO gas partial pressures could be recorded. Measured PO_2 values in the ABO ranged from 5.8 to 15.6 kPa oxygen, while PCO_2 values typically were in the range of 1.95–3.89 kPa. When the PO_2 in the air space was reduced to 13.6–14.6 kPa (aerial hypoxia; achieved due to the oxygen uptake of the fish and only partial renewal of the air), measured PO_2 in the ABO was in the range of 4.87–8.76 kPa, while PCO_2 values were in the range of 2.92–4.87 kPa (Fig. 3b). Plotting PO_2 values of the ABO against the time difference between the last air breath and the time of measurement of ABO PO_2 revealed a clear decrease in ABO PO_2 with time, and this was observed under aerial normoxia (Fig. 4a) as well as under aerial hypoxia (Fig. 4b).

Breath volume under normoxic conditions in the air space ($P_IO_2 > 18$ kPa) and also under hypoxic conditions

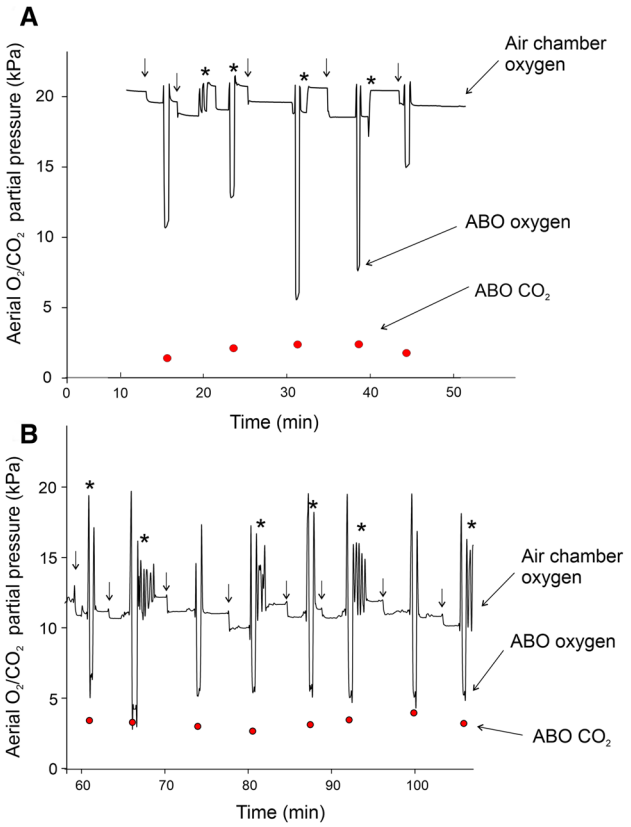

Fig. 3 **a** Air chamber O_2 partial pressure during individual air-breaths as well as ABO O_2 and CO_2 partial pressure recorded after an air-breath in a large *A. gigas* (body mass 470 g) during aerial normoxia (O_2 partial pressure 18–20 kPa), in Series 1. After taking a gas sample from the ABO the PO_2 microsensor was removed from the air chamber and used to measure gas partial pressure in the ABO gas sample, together with the PCO_2 microsensor. To avoid hypoxia air chamber gas was repeatedly renewed by frequent flushing with air. Immediately after recording ABO gas partial pressures the PO_2 microsensor was returned to the air chamber to record the next breath. Vertical arrows indicate taking of an air breath; *flushing of the air chamber to stabilize aerial PO_2. **b** Air chamber O_2 content during individual air-breaths and ABO O_2 and CO_2 content recorded after an air-breath in a large *A. gigas* (body mass 660 g) during air-chamber hypoxia (O_2 partial pressure 12–14 kPa). Air chamber hypoxia was achieved by allowing repeated breaths without flushing the air chamber. After reaching hypoxia in the air chamber the PO_2 was stabilized at a value of 12–14 kPa by careful partial renewal of the air chamber gas. Vertical arrows indicate taking of an air breath; *flushing of the air chamber to stabilize aerial PO_2

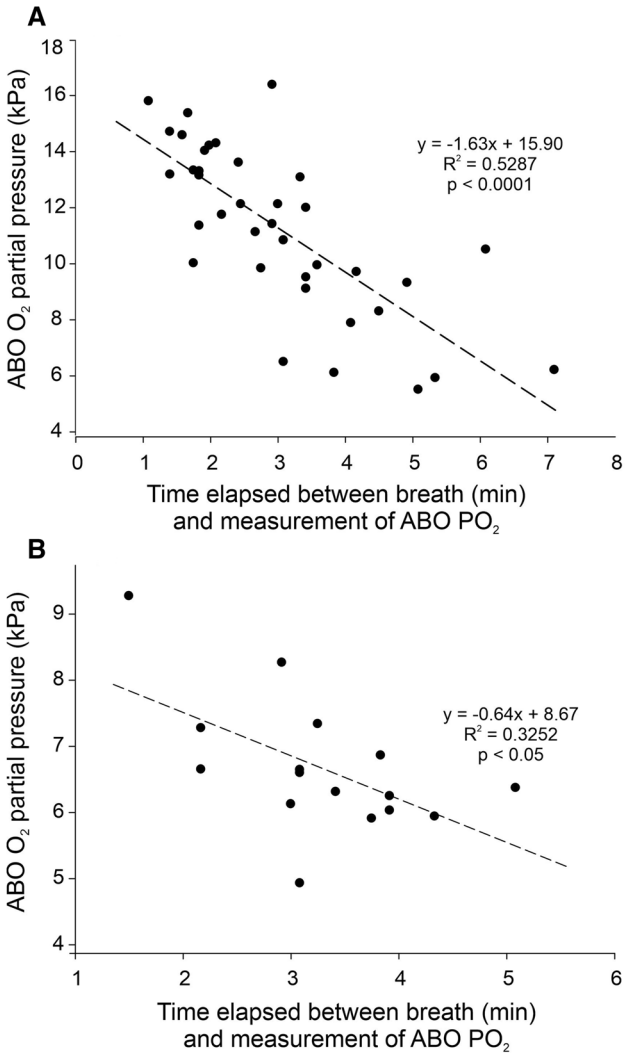

Fig. 4 Time elapsed after the air-breath plotted versus the ABO O_2 partial pressure (**a**) during aerial normoxia (air-chamber O_2 partial pressure 18–20 kPa) and during (**b**) aerial hypoxia (air-chamber O_2 partial pressure 10.6–14.6 kPa), in Series 1. Data collected from six experiments using three different fish. Regression lines, R^2 values, and p values are shown

($P_IO_2 = 13.42 \pm 0.27$ kPa) was quite variable, typically ranging from about 20 to 130 mL kg^{-1}. Calculation of breath volume is based on the measurement of the ABO PO_2. Air breaths are taken at irregular intervals and, therefore, measurement of ABO PO_2 did not occur just prior to taking an air breath, so that the actual PO_2 in the ABO at the time of air breathing was determined by extrapolation based on the decrease of ABO PO_2 with time, as determined in Fig. 4. This certainly contributed to the variability of the calculated breath volume. Plotting breath volume versus the extrapolated PO_2 in the ABO under normoxic conditions revealed a significant correlation between the volume of the breath and ABO PO_2 (Fig. 5a), the lower breath volume the lower was ABO PO_2. Under hypoxic conditions, however, no correlation between breath volume and ABO PO_2 was detected. There was no significant difference in breath volume between hypoxic and normoxic values (Fig. 5b).

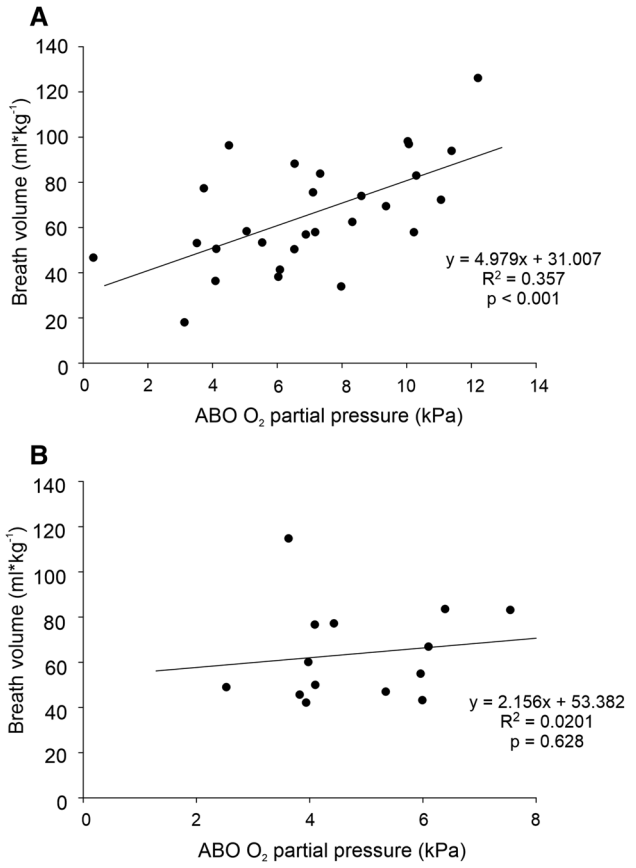

Fig. 5 Breath volume in relation to the O_2 partial pressure of the ABO, extrapolated from the time of measurement to the next air breath based on the regression analysis presented in Fig. 4, during (**a**) normoxia (air-chamber O_2 partial pressure 18–20 kPa) and during (**b**) aerial hypoxia (air-chamber O_2 partial pressure 10.6–14.6 kPa) in Series 1. Data collected from six experiments using three different fish. Regression lines, R^2 values, and p values are shown

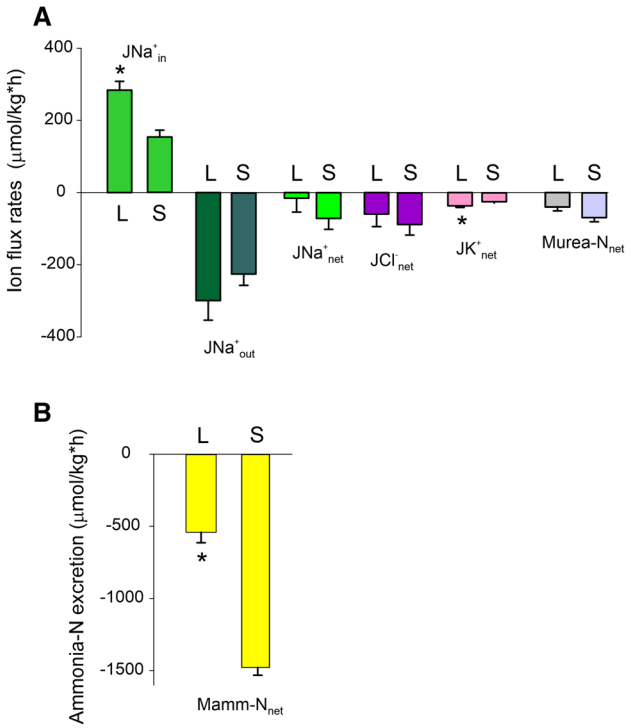

Fig. 6 A comparison between large (L) (619.2 ± 53.8 g, $N = 6$) and small (S) (20.44 ± 0.43 g. $N = 28$) *A. gigas* of (**a**) mass-specific rates of sodium influx (J_{in}^{Na+}), efflux (J_{out}^{Na+}), and net flux (J_{net}^{Na+}), as well as net flux rates of chloride (J_{net}^{Cl-}), potassium (J_{net}^{K+}), and urea-N excretion ($M_{urea\text{-}N}$), and **b** mass-specific rates of ammonia-N excretion ($M_{amm\text{-}N}$) in Series 2. Means ± SEM. *Significant differences between small and large fish, $p < 0.05$

Series 2

Ionic exchange and N-waste excretion in large versus small pirarucu

In this comparison (Fig. 6), the small pirarucu were approximately 20 g in mass—i.e. fourfold larger than the small fish of Series 1, whereas the large pirarucu were very similar in size (600–700 g) to those of Series 1. In the small fish, mass-specific unidirectional sodium influx rate (J_{in}^{Na+}, + 153.4 ± 19.0 µmol kg^{-1} h^{-1}) was significantly lower than in the large fish (+ 283.8 ± 24.3 µmol kg^{-1} h^{-1}) (Fig. 6a), very different from the opposite patterns of the metabolic parameters seen in the comparison of Series 1 (cf. Table 1). Sodium efflux (J_{out}^{Na+}) and net flux rates (J_{net}^{Na+}), as well as chloride net flux rates (J_{net}^{Cl-}) were not significantly different between small and large *A. gigas*, but potassium net flux rates (J_{net}^{K+}) were also lower in the small fish (− 24.6 ± 4.0 µmol kg^{-1} h^{-1}) than in the large animals (− 36.8 ± 4.4 µmol kg^{-1} h^{-1}) (Fig. 6a).

As in the 5-g fish of Series 1, high mass-specific ammonia-N excretion rates ($M_{amm\text{-}N}$) were still seen in the 20-g fish of Series 2 (1478 ± 53 µmol kg^{-1} h^{-1}) though they had fallen somewhat, whereas the rates in the large pirarucu (541 ± 72 µmol kg^{-1} h^{-1}) were very similar to those recorded in Series 1 (Fig. 6b, cf. Table 1). However, by 20-g, the mass-specific urea-N excretion rates ($J_{urea\text{-}N}$) had dropped precipitously from the high rates seen in the 5-g fish, whereas the rates in the large fish were very similar to those of Series 1. $M_{urea\text{-}N}$ values were no longer different between small (− 68.6 ± 7.3 µmol kg^{-1} h^{-1}) and large *A. gigas* (− 40.0 ± 10.7 µmol kg^{-1} h^{-1}) (Fig. 6a).

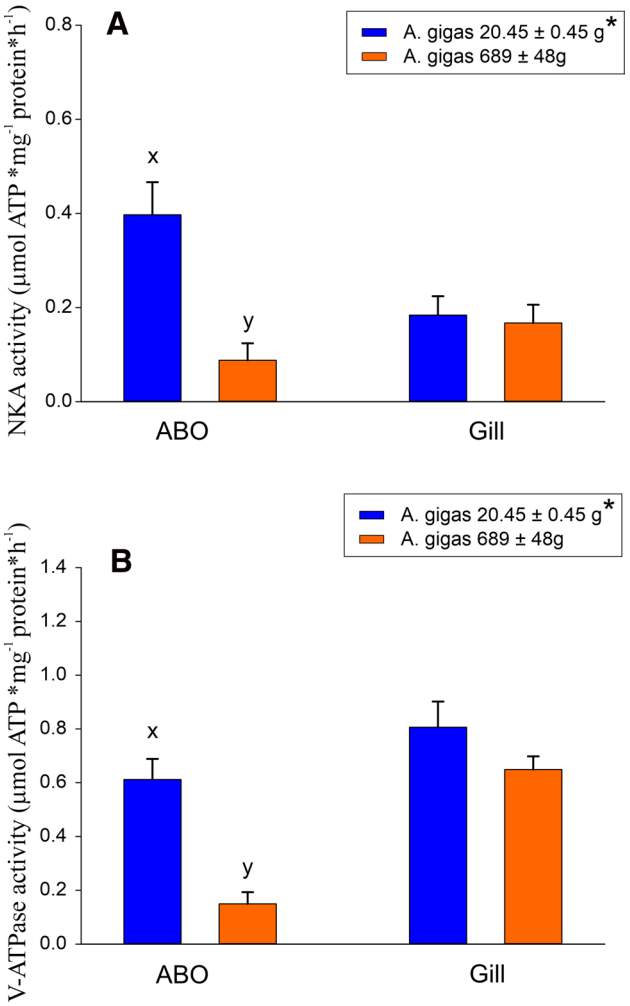

Fig. 7 Na^+, K^+-ATPase (NKA) (**a**) and V-type H^+ ATPase (**b**) activity in small and large *A. gigas* gill tissue and ABO. *Significant overall differences between small and large fish; different small letters denote significant differences between small and large *A. gigas* at the tissue level. Means ± SEM ($N = 7$; $p < 0.05$)

Series 3

Branchial and ABO enzyme activities in large versus small pirarucu

Na^+, K^+-ATPase (NKA) activity measured in gill tissue of small (20-g, from Series 2) and large individuals (600–700-g, from Series 1) of *A. gigas* was not significantly different, but in small fish the activity was significantly higher in the ABO than in large fish (Fig. 7a). V-type H^+ATPase activity was three- to fourfold higher than NKA activity in gill tissue of both small and large *A. gigas*. As with NKA, V-type H^+ ATPase in the ABO of small fish was significantly higher than in large fish (Fig. 7b). Overall, the all pairwise multiple comparisons (Holm–Sidak post hoc test) revealed that in small fish the enzyme activities were higher than in large fish.

Discussion

The influence of development on O_2 uptake, CO_2 excretion, N-waste excretion, and ionoregulation

Arapaima gigas is the largest freshwater fish in the Amazon and grows very quickly in the first year. While after hatching the fish have normal gills with gill filaments and lamellae, during early development the gill lamellae rapidly disappear, resulting in a significant reduction in branchial diffusion capacity (Brauner et al. 2004; Fernandes et al. 2012; Gonzalez et al. 2010). The decrease in diffusion capacity is expected to impair gill O_2 uptake, and with proceeding development *A. gigas* becomes an obligate air-breathing fish. Our data now reveal that even the smallest stages with only 4–6 g body mass, which do have typical gills with filaments and lamellae, frequently breathe air and take up more O_2 from the air than from the water. Air-breathing frequency was even higher in small fish (every 3.31 min) as compared to large fish. Air-breathing frequencies observed for larger fish with a breath every 5.58 min are slightly lower than reported in previous studies, where a breath has been recorded every 4.2 or 4 min for 2 kg *A. gigas* (Farrell and Randall 1978; Randall et al. 1978), while Stevens and Holeton observed a breath even every 1–2 min at temperatures similar to those used in our study (Stevens and Holeton 1978).

The fraction of aerial O_2 uptake recorded for large *A. gigas* was with 75 ± 2% well within the range reported in previous studies on fish ranging from 70 g to 3 kg (Brauner and Val 1996; Gonzalez et al. 2010; Stevens and Holeton 1978). The value obtained for small *A. gigas* (63 ± 3%) was significantly lower than in larger fish, but much higher than expected, in contrast to our first hypothesis. We did, however, confirm our prediction that it would be necessary to look at very small fish to see the greater reliance on water-breathing, in this case 4–6 g, much smaller than the 70-g fish used by Gonzalez et al. (2010). Although the O_2 exchange capacity of the gills in small fish is much higher than in the large fish, they mostly rely on aerial respiration. Thus, even in small *A. gigas*, gills are of minor importance for O_2 uptake. Our data thus indicate that development beyond 4–5 g appears to have only a small effect on O_2 uptake. A body mass of about 10 g is reached within 4 weeks after hatching (Brauner and Val 2006); therefore, soon after hatching aerial respiration is the main source for O_2. In future, it will be of interest to see if there is any stage post-hatch where the gills are predominant in O_2 uptake.

Gills are, however, the main site for CO_2 excretion. In large fish, the fraction of CO_2 excreted into the air was with 12 ± 1%, much lower than the 36.9% reported by Randall et al. (1978) but comparable to the 11–15% reported by Brauner and Val (1996) and Gonzalez et al. (2010) in 70–1700 g *A. gigas*. Considering this rate of aerial CO_2 excretion in context with the amount of O_2 taken up from the air, we calculated an aerial respiratory exchange ratio of 0.23 for large *A. gigas*. This value compares to values between 0.14 and 0.36, calculated from lung gas measurements in fish of about 2 kg body mass (Randall et al. 1978).

In small *A. gigas*, CO_2 was almost exclusively excreted via the gills. The fraction of aerial CO_2 excretion in small fish was only 3%, much smaller than in large fish (12%), and this low rate of aerial CO_2 excretion was also reflected in the low respiratory exchange ratio of 0.07. Due to the high solubility of CO_2 in water, water breathers have much lower arterial PCO_2 values than air-breathing animals (Bayley et al. 2018; Howell 1970; Rahn 1966). Accordingly, switching to aerial respiration results in an increase in blood PCO_2, and arterial PCO_2 values in air-breathing fish typically are much higher than in water-breathing fish (Graham 1997; Perry et al. 2005). For *A. gigas*, it has been shown that arterial PCO_2 values increase with development. Gonzalez et al. (2010) reported that in fish of about 70 g, the average PCO_2 of blood obtained by caudal puncture was 16.5 mmHg (2.2 kPa), while in fish of about 720 g, the PCO_2 was 26.2 mm Hg (3.49 kPa). In *A. gigas* of only 4–5 g, therefore, a PCO_2 far below 16.5 mm Hg (2.2 kPa) can be expected, which probably is too low to allow for a substantial rate of aerial CO_2 excretion. In contrast to O_2, our data indicate that on a relative basis, the route of CO_2 excretion is affected to a much greater extent by development beyond 4–6 g. The data available so far suggest that starting from the water exposed hatchling, the elevation of arterial PCO_2 slowly occurs with proceeding development, finally allowing for about 12–15% aerial CO_2 excretion. According to Gonzalez et al. (2010), this stage is already reached at a body mass of about 67 g. The relative contribution of aerial CO_2 excretion (14.3%) of 67 g fish was even slightly higher than that of fish with a tenfold higher body mass (11%).

There were marked changes in N-waste excretion associated with development. In 4–6 g pirarucu, $M_{urea\text{-}N}$ accounted for 19% of total N-excretion, but this had dropped to 4.5% at 20 g and 8% at 600–700 g, similar to the 8% reported for both 70 g and 600–700 g individuals by Gonzalez et al. (2010). We attribute this decline to the shutting down of urea-N production by the ornithine–urea cycle (OUC), which is very active in the early life stages of most teleosts, a pattern which has been seen in many other species (Wright and Fyhn 2001; Zimmer et al. 2017). In virtually all teleosts, the OUC is shut down as development proceeds into adult life, apart from a few notable exceptions such as the Magadi tilapia and several toadfish (reviewed by Wood 1996). As ammonia-N excretion predominated in both small (4–6 g) and large (600–700 g) *A. gigas*, $M_{amm\text{-}N}$ and $M_{total\text{-}N}$ declined more or less in proportion as development proceeded, and in approximate parallel to the decline in mass-specific MO_{2total}. As a result, the NQ did not change significantly (0.22 in small, 0.16 in large fish). Using standard metabolic theory (Kleiber 1965; Lauff and Wood 1996), we can combine these NQ values with the fractional urea-N excretion (0.19 in small, 0.08 in large) and the measured RQ values (0.72 in small, 0.91 in large fish, again not significantly different), to estimate relative aerobic usage of metabolic fuels. This yielded values of 81.5% protein and 18.5% lipid in small fish versus 60.6% protein, 16.2% carbohydrate, and 23.2% lipid in large fish. Given the non-significant differences in NQ and RQ values, we cannot conclude that these fuel usages differ. However, the important point is that both size classes are burning an unusually high percentage (60.6–81.5%) of protein in oxidative metabolism, despite the fact that they were fasting during measurements. Most fasting teleosts tend to conserve protein, with generally less than 35% of aerobic metabolism depending on this fuel (Wood 2001). However, we have recently found that several other Amazonian fish also rely heavily on protein oxidation during fasting (Pelster et al. 2015; Wood et al. 2016). From the data of Gonzalez et al. (2010), we can estimate similarly high NQ values (0.21–0.36) and protein oxidation (77–100%) for their 70–700 g *A. gigas*, which are avid carnivores. Nitrogen turnover thus appears to be very high in both small and large *A. gigas*, in spite of the rapid growth rate.

Unidirectional sodium influx (J_{in}^{Na+}) and potassium net loss (J_{net}^{K+}) were the only ion flux rates in which mass-specific values were significantly higher in large versus small *A. gigas*. The differences were approximately 1.5–2-fold between 20 and 700-g fish. This finding agrees qualitatively with the report of Gonzalez et al. (2010) of approximately threefold higher mass-specific J_{in}^{Na+} and J_{out}^{Na+} values in 700- versus 70-g *A. gigas*. J_{out}^{Na+} values were also higher in our large fish, but the difference was not significant. We ensured that pre-measurement conditions were the same in our large and small fish, so the differences appear to be inherent. Nevertheless, these results are surprising, and contrary to our hypothesis that all gill-dependent processes would scale with body mass in a similar fashion, especially in light of the reduction in gill surface area and increased water-to-blood diffusion distance with growth (Brauner et al. 2004; Fernandes et al. 2012; Gonzalez et al. 2010), and the lack of change in branchial Na^+, K^+-ATPase and V-type H^+ ATPase activities with size in our fish (see below). Gonzalez et al. (2010) actually measured 48% lower gill Na^+,

K^+-ATPase in large versus small pirarucu, despite the higher flux rates in the former.

As pointed out by Brauner et al. (2004) and Ramos et al. (2013), a morphological explanation for this anomaly may lie in the marked proliferation of mitochondria-rich cells (MRCs) on the reduced branchial surface of larger *A. gigas*, observed in both these studies. In addition, Ramos et al. (2013) reported that exposed fractional surface area of the MRCs (presumed sites of active ion uptake) increased greatly, and paracellular channels (presumed sites of diffusive ion losses) became larger and deeper with growth. But why should larger pirarucu need higher ion flux rates? Perhaps it relates to acid–base balance that is likely to be coupled to gill ion exchange (Pelster and Wood 2018). To regulate blood pH, larger animals relying on air-breathing to a greater extent must retain more [HCO_3^-] to balance their higher blood PCO_2 levels. Indeed, when subjected to an experimental respiratory acidosis, large pirarucu were able to regulate blood pH more effectively than small animals (Gonzalez et al. 2010). But this species also has a very large and well-developed kidney (Fernandes et al. 2012; Hochachka et al. 1978). In future studies, it will be of interest to quantify the relative roles of gills and kidney in correcting ion and acid–base disturbances in this species.

The differences discussed above between large and small *A. gigas* were well illustrated by the calculated mass-scaling exponents (Table 2). Notably, we did not see a difference in the scaling of $M_{amm\text{-}N}$ versus MO_{2total}, in contrast to Gonzalez et al. (2010). We had hypothesized that scaling coefficients would be fairly uniform for those processes depending mainly on gill function. This was confirmed for MO_{2water}, MCO_{2water}, MCO_{2total}, $M_{amm\text{-}N}$, $M_{urea\text{-}N}$, and $M_{total\text{-}N}$ (hypo-allometric values between 0.70 and 0.84). However, the hyper-allometry of J_{in}^{Na+} (1.27) and J_{out}^{Na+} (1.06) was remarkable. For net K^+ loss rate (J_{net}^{K+}), a similarly high scaling coefficient (1.18) could be estimated only from the means, because the contributions of both positive and negative values prevented calculations based on individual fish. It is also notable that the fourfold increase in the fractional contribution of the ABO to MCO_2 (Table 1) was reflected in a hyper-allometric coefficient for MCO_{2air} (1.12), in contrast to 0.82–0.84 for MCO_{2water} and MCO_{2total} (Table 2).

Table 2 Allometric scaling coefficients calculated for respiratory, metabolic, and ionoregulatory rates measured in small and large *A. gigas* of Series 1 and 2

	Coefficient	*N*	R^2
MO_{2air}	0.790 ± 0.068^{AB}	16	0.952
MO_{2water}	0.700 ± 0.031^{A}	17	0.985
MO_{2total}	0.776 ± 0.045^{AB}	15	0.980
MCO_{2air}	1.124 ± 0.067^{C}	15	0.979
MCO_{2water}	0.823 ± 0.047^{B}	15	0.981
MCO_{2total}	0.843 ± 0.046^{B}	15	0.983
$M_{amm\text{-}N}$	0.724 ± 0.027^{AB}	50	0.724
$M_{urea\text{-}N}$	0.730 ± 0.070^{AB}	50	0.693
$M_{total\text{-}N}$	0.718 ± 0.027^{AB}	50	0.972
J_{in}^{Na}	1.265 ± 0.121^{C}	30	0.900
J_{out}^{Na}	1.058 ± 0.134^{BC}	30	0.837
J_{net}^{Na}	0.554[a]		
J_{net}^{Cl}	0.887[a]		
J_{net}^{K}	1.118[a]		

Means sharing the same letter are not significantly different

Means ± 1 SEM

[a]Calculated from size-group means—see text for details

Gas composition in the air-breathing organ of large pirarucu and the response to aerial hypoxia

PO_2 values measured in the ABO were quite variable in normoxia, ranging from 5.84 to 15.6 kPa, while PCO_2 varied between 1.95 and 3.89 kPa. Gas samples from the ABO were collected at different times post-breath, which certainly contributed to this variability, because ABO PO_2 decreased with time after the last air breath. Recordings of ABO gas partial pressures in fish of about 2 kg body mass after an air-breath showed a PO_2 decrease from 140 down to 80 mmHg (18.7–10.7 kPa), while PCO_2 increased from about 16 to 35 mmHg (2.13–4.67 kPa) (Randall et al. 1978). The data on ABO PCO_2 are near the PCO_2 value of about 26 mmHg (3.47 kPa) measured in blood samples of large *A. gigas* (Gonzalez et al. 2010; Randall et al. 1978). PCO_2 in the ABO thus appears to be close to blood PCO_2. Given the rich vascularization, the short measured diffusion distances between gas space and blood and the high diffusion capacity calculated for the ABO (Fernandes et al. 2012), a rapid equilibration between blood gases and ABO gases is quite likely. The PO_2 in the ABO decreased with time after the last air breath, demonstrating that O_2 was continuously removed from the ABO. Compared to O_2, the CO_2 exchange rate of the ABO remained low, and the gills remained the main site of CO_2 exchange. This certainly can be attributed to the high solubility of CO_2 in water, which facilitates aquatic CO_2 excretion. Another important factor appears to be the low ventilation frequency (once every 5–6 min), which with a rapid equilibration of blood PCO_2 and ABO PCO_2 probably contributed to high ABO PCO_2 values. High ABO PCO_2 values, however, imply that the difference between blood PCO_2 and ABO PCO_2 remains small.

O_2 uptake from the ABO by far exceeded aerial CO_2 excretion, which should result in a decrease in ABO volume between two subsequent air breaths. *A. gigas* exhales first, and filling the ABO with air is achieved by suction, supported by the buccal pump (Farrell and Randall 1978), although this has been refuted by Greenwood and Liem

(1984). It is assumed that the ventral membrane of the ABO may act as a diaphragm-like septum and create the suction for inhalation (Farrell and Randall 1978; Fernandes et al. 2012). In consequence, muscular activity influences ABO volume and therefore removal of O_2 from the ABO may result in a volume decrease, but it may also result in a decrease in pressure. Farrell and Randall (1978) reported that ABO pressure in submerged *A. gigas* remained constant at slightly above atmospheric levels, independent of the diving depth of the fish. Based on the gas laws, this observation suggests that the volume of the ABO should slowly decrease because O_2 is continuously removed, while CO_2 is excreted mainly via the gills and not via the ABO, but it also suggests that ABO pressure and/or volume are controlled and can be regulated.

It has been estimated that ABO volume would be about 10% of body volume (Fernandes et al. 2012; Randall et al. 1978). Breath volumes calculated from our results thus suggest that a substantial fraction of the ABO volume is exchanged with each breath. From gas samples taken before and after a breath, it has been estimated that breath volume is about 70% of ABO volume (Randall et al. 1978). This is supported by our data which, assuming that ABO volume is about 10% of body volume, suggested an average breath volume of 60–70% of ABO volume. The large breath volume exchanged within milliseconds clearly supported the conclusion that muscular activity is involved in air breathing. The comparatively large breath volume appears necessary because a breath is taken only every few minutes. Our data clearly show that breath volume correlates with ABO PO_2, and smaller breath volumes are associated with much lower ABO PO_2 values. This would reduce the partial pressure gradient between gas phase and the blood and impair gas exchange in the ABO.

Aquatic hypoxia is one of the factors possibly driving the development of air-breathing, and hypoxia has, for example, been shown to stimulate air-breathing in the jeju, *Hoplerythrinus unitaeniatus* (Pelster et al. 2016). A reduction in aerial PO_2, i.e. aerial hypoxia, significantly reduced ABO PO_2, but it did not stimulate air-breathing in *A. gigas*, as reported for several obligatory air-breathing fish (see Perry et al. 2009). The time between subsequent air-breaths was not reduced, in either small or in large fish. In a previous study, ABO PO_2 was experimentally modified by replacing gas of the ABO with different gas mixtures, and the results also indicated that breathing rate was influenced by ABO PO_2 (Farrell and Randall 1978). These experiments, however, were performed with few fish and a quantitative analysis of the results was not possible. We observed that fish started to struggle if aerial PO_2 was below 11 kPa and therefore avoided lower PO_2 values. While the present data do not support our hypothesis that aerial hypoxia would stimulate air-breathing, it is quite possible that conditions with much lower or much higher PO_2 values in the ABO than experienced in our experiments will affect air-breathing frequency and/or breath volume.

Our data clearly show that the gills are the almost exclusive site of CO_2 excretion in small *A. gigas*, and remain the main site of CO_2 excretion in large fish. CO_2 excretion is closely related to ion exchange, and gill tissue is characterized by high activities of ATPases, providing the energy for ion transport processes. NKA activities measured in gill tissue of *A. gigas* on the Alpha Helix expedition varied between 0.03 and 0.04 µmol h^{-1} g^{-1} wet wt. (Hochachka et al. 1978; Hulbert et al. 1978), and this was about 4-times lower than the activity recorded from purely water breathing osteoglossid fish. Gonzalez et al. (2010) compared NKA activity in gill tissue of 67-g and 724-g *A. gigas*. In that study, NKA activity in gills of the 67-g fish (0.42 µmol h^{-1} mg^{-1} protein) was significantly higher than in the larger fish (0.22 µmol h^{-1} mg^{-1} protein). These values fit well to our NKA measurements, but we did not see a significant difference in the NKA activity in gill tissue of small and larger *A. gigas*. We also measured V-type H^+ ATPase activity in gill tissue, and this activity was three- to fourfold higher than NKA activity, and again, there was no difference between the two developmental stages. ATPase activities measured by the same techniques in gill tissue of the facultative air-breathing jeju, *Hoplerythrinus unitaeniatus* (Wood et al. 2016), were about tenfold higher than in *A. gigas*, and mass-specific values of J_{in}^{Na+} and J_{out}^{Na+} were about twofold higher (Cameron and Wood 1978) supporting the conclusion that the ion transport capacity of gills of *A. gigas* is generally low.

We were surprised to find that in the ABO, which cannot contribute to normal ion exchange with the water, activities of these two ATPases were in a similar range as in gill tissue. In the ABO of larger fish, both activities were significantly reduced as compared to the small fish. The ABO is derived from the esophagus (Graham 1997), and the high activity recorded in the early stage fish may be related to the origin of the tissue. We speculate that ion transport in the ABO may have an important functional role by rapidly removing small amounts of water from the ABO surface (through osmotic attraction into the blood) that may be inadvertently swallowed during air-breathing. We observed several instances of drowning by water inhalation when fish were recovering from anesthesia. As development proceeds, this may become less of a problem, so the activities of the two ATPases can be reduced.

In conclusion, our data reveal that the reduction in gill gas exchange capacity hardly affected O_2 uptake, as even in 4–6 g fish, a size reached about 2–3 weeks after hatching (Brauner and Val 2006), most of the O_2 is taken up by aerial respiration. CO_2 excretion, however, is significantly affected. At this stage, CO_2 is almost exclusively excreted via the gills, and with a slow increase in blood PCO_2 during

development, finally about 12–15% of the CO_2 can be eliminated via the ABO. Nevertheless, the gills retain their role as the main site for CO_2 excretion, and probably also for ammonia-N and urea-N excretion, though this remains to be confirmed as Gonzalez et al. (2010) reported quite high concentrations of these two N-wastes in spot-samples of urine of *A. gigas*. Most rate functions show fairly similar hypoallometry with scaling, but we confirm the finding of Gonzalez et al. (2010) that mass-specific rates of ion-exchange actually increase with body size despite the decrease in relative gill surface area. This trend is perhaps associated with increasing requirements for acid–base regulation as the animal relies more on air-breathing as it grows. Nevertheless, the comparatively low absolute activities of branchial ion-transport ATPase enzymes and low ion-exchange rates suggest an overall low capacity for ion exchange in this obligate air-breather. This supports the hypothesis that the peculiar arrangement of the kidney, which due to its location inside the ABO is in intimate contact to air (Fernandes et al. 2012; Hochachka et al. 1978), may have adopted a more important role for ion and acid–base homeostasis.

Acknowledgements Financial support by INCT ADAPTA-CNPq (465540/2014-7)/FAPEAM (062.1187/2017)/CAPES (finance code 001), Science without Borders (Brazil), and NSERC Discovery (Canada) (RGPIN-2017-03843) is gratefully acknowledged. ALV is the recipient of a research fellowship from Brazilian CNPq. We thank Drs. Raul Suarez and John Onukwufor for advice on allometry calculations. This research was made possible by the generous gift of prototype PCO_2 micro-fibre-optodes, opto-electronic meter, and software by PreSens Precision Sensing GmbH. We thank Fernando Martinez Ferreras, Miriam Ubach Granados, and Laura Perez Medina of PreSens Precision Sensing GmbH for advice and support.

References

Bartlett GR (1980) Phosphate compounds in vertebrate red blood cells. Am Zool 20:103–114

Bayley M, Damsgaard C, Thomsen M, Malte H, Wang T (2018) Learning to air-breathe: the first steps. Physiology 34(1):14–29

Boutilier RG, Heming TA, Iwama GK (1984) Appendix: physicochemical parameters for use in respiratory physiology. In: Hoar WS, Randall DJ (eds) Fish physiology. Academic Press, Orlando, pp 403–430

Bradford MM (1976) A rapid and sensitive method for the quantitation of microgram quantities of protein utilizing the principle of protein-dye binding. Anal Biochem 72:248–254

Brauner CJ, Val AL (1996) The interaction between O_2 and CO_2 exchange in the obligate air-breather Arapaima gigas, and the facultative air breather, Lipossarcus pardalis. In: Val AL, Almeida-Val V, Randall DJ (eds) Physiology and biochemistry of the fishes of the Amazon. INPA, Manaus, pp 101–110

Brauner CJ, Val AL (2006) Oxygen transfer. In: Val AL, Almeida-Val VMF, Randall DJ (eds) The physiology of tropical fishes. Academic Press, Amsterdam, pp 277–306

Brauner CJ, Matey V, Wilson JM, Bernier NJ, Val AL (2004) Transition in organ function during the evolution of air-breathing; insights from *Arapaima gigas*, an obligate air-breathing teleost from the Amazon. J Exp Biol 207(9):1433–1438

Cameron JN, Wood CM (1978) Renal function and acid-base regulation in two Amazon erythrinid fishes: *Hoplias malabaricus*, a water breather, and *Hoplerythrinus unitaeniatus*, a facultative air breather. Can J Zool 56:917–930

Damsgaard C, Baliga VB, Bates E, Burggren W, McKenzie DJ, Taylor E, Wright PA (2019) Evolutionary and cardio-respiratory physiology of air-breathing and amphibious fishes. Acta Physiol 228(3):e13406

Dejours P (1981) Principles of comparative respiratory physiology, 2nd edn. Elsevier, Amsterdam

Diaz RJ, Breitburg DL (2009) The hypoxic environment. In: Richards JG, Farrell AP, Brauner CJ (eds) Hypoxia. Elsevier, Amsterdam, pp 1–23

Farrell AP, Randall DJ (1978) Air-breathing mechanics in two Amazonian teleosts, *Arapaima gigas* and *Hoplerythrinus unitaeniatus*. Can J Zool 56:939–945

Fernandes MN, da Cruz AL, da Costa OTF, Perry SF (2012) Morphometric partitioning of the respiratory surface area and diffusion capacity of the gills and swim bladder in juvenile Amazonian air-breathing fish, *Arapaima gigas*. Micron 43(9):961–970

Forgac M (1989) Structure and function of vacuolar class of ATP-driven proton pumps. Physiol Rev 69:765–796

Gonzalez RJ, Brauner CJ, Wang YX, Richards JG, Patrick ML, Xi W, Matey V, Val AL (2010) Impact of ontogenetic changes in branchial morphology on gill function in *Arapaima gigas*. Physiol Biochem Zool 83(2):322–332

Graham JB (1997) Air-breathing fishes. Evolutions, diversity, and adaptation. Academic Press, London, pp 1–299

Greenwood PH, Liem KF (1984) Aspiratory respiration in *Arapaima gigas* (Teleostei, Osteoglossomorpha): a reappraisal. J Zool 203(3):411–425

Hochachka PW, Moon TW, Bailey J, Hulbert WC (1978) The osteoglossid kidney: correlations of structure, function, and metabolism with transition to air breathing. Can J Zool 56:820–832

Howell BJ (1970) Acid-base balance in transition from water breathing to air breathing. Fed Proc 29:1130–1134

Hulbert WC, Moon TW, Hochachka PW (1978) The osteoglossid gill: correlations of structure, function, and metabolism with transition to air breathing. Can J Zool 56:801–808

Isaacks RE, Kim HD, Bartlett GR, Harkness DR (1977) Inositol pentaphosphate in erythrocytes of a freshwater fish, piraracu (*Arapaima gigas*). Life Sci 20(6):987–990

Ishimatsu A (2012) Evolution of the cardiorespiratory system in air-breathing fishes. Aqua-BioSci Monogr 5:1–28

Johansen K, Mangum CP, Weber RE (1978) Reduced blood O_2 affinity associated with air breathing in osteoglossid fishes. Can J Zool 56(4):891–897

Kleiber M (1965) Respiratory exchange and metabolic rate. Handbook of physiology. Respiration, vol 3. American Physiological Society, Washington, pp 927–937

Kültz D, Somero GN (1995) Osmotic and thermal effects on in situ ATPase activity in permeabilized gill epithelial cells of the fish *Gillichthys mirabilis*. J Exp Biol 198:1883–1894

Lauff RF, Wood CH (1996) Respiratory gas exchange, nitrogenous waste excretion, and fuel usage during aerobic swimming in juvenile rainbow trout. J Comp Physiol B 166:501–509

Lee DJ, Gutbrod M, Ferreras FM, Matthews PGD (2018) Changes in hemolymph total CO_2 content during the water-to-air respiratory transition of amphibiotic dragonflies. J Exp Biol 221(15):181438

Muusze B, Marcon J, Van den Thillart G, Almeida-Val V (1998) Hypoxia tolerance of Amazon fish respirometry and energy metabolism of the cichlid *Astronotus ocellatus*. Comp Biochem Physiol Part A 120:151–156

Nawata CM, Hung CCY, Tsui TKN, Wilson JM, Wright PA, Wood CM (2007) Ammonia excretion in rainbow trout (*Oncorhynchus mykiss*): evidence for Rh glycoprotein and H+-ATPase involvement. Physiol Genomics 31:463–474

Pelster B, Wood CM (2018) Ionoregulatory and oxidative stress issues associated with the evolution of air-breathing. Acta Histochem 120(7):667–679

Pelster B, Wood CM, Speers-Roesch B, Driedzic WR, Almeida-Val V, Val A (2015) Gut transport characteristics in herbivorous and carnivorous serrasalmid fish from ion-poor Rio Negro water. J Comp Physiol B 185(2):225–241

Pelster B, Giacomin M, Wood CM, Val AL (2016) Improved ROS defense in the swimbladder of a facultative air-breathing erythrinid fish, jeju, compared to a non-air-breathing close relative, traira. J Comp Physiol B 186(5):615–624

Pelster B, Wood CM, Jung E, Val AL (2018) Air-breathing behavior, oxygen concentrations, and ROS defense in the swimbladders of two erythrinid fish, the facultative air-breathing jeju, and the non-air-breathing traira during normoxia, hypoxia and hyperoxia. J Comp Physiol B 188(3):437–449

Perry SF, Gilmour KM, Swenson ER, Vulesevic B, Chew SF, Ip YK (2005) An investigation of the role of carbonic anhydrase in aquatic and aerial gas transfer in the African lungfish *Protopterus dolloi*. J Exp Biol 208(19):3805–3815

Perry SF, Jonz MG, Gilmour KM (2009) Oxygen sensing and the hypoxic ventilatory response. In: Richards JG, Farrell AP, Brauner CJ (eds) Hypoxia. Academic Press, Amsterdam, pp 193–253

Rahmatullah M, Boyde TR (1980) Improvements in the determination of urea using diacetyl monoxime; methods with and without deproteinisation. Clin Chim Acta 107:3–9

Rahn H (1966) Aquatic gas exchange: theory. Respir Physiol 1(1):1–12

Ramos CA, Fernandes MN, da Costa OTF, Duncan WP (2013) Implications for osmorespiratory compromise by anatomical remodeling in the gills of *Arapaima gigas*. Anat Rec 296(10):1664–1675

Randall DJ, Farrell AP, Haswell MS (1978) Carbon dioxide excretion in the pirarucu (*Arapaima gigas*), an obligate air-breathing fish. Can J Zool 56:977–982

Randall DJ, Cameron JN, Daxboeck C, Smatresk N (1981) Aspects of bimodal gas exchange in the bowfin, *Amia calva* L. (Actinopterygii: Amiiformes). Respir Physiol 43(3):339–348

Scott GR, Matey V, Mendoza JA, Gilmour KM, Perry SF, Almeida-Val VMF, Val AL (2017) Air breathing and aquatic gas exchange during hypoxia in armoured catfish. J Comp Physiol B 187(1):117–133

Shartau RB, Brauner CJ (2014) Acid–base and ion balance in fishes with bimodal respiration. J Fish Biol 84(3):682–704

Smatresk NJ (1986) Ventilatory and cardiac reflex responses to hypoxia and NaCN in *Lepisosteus osseus*, an air-breathing fish. Physiol Zool 59(4):385–397

Smatresk NJ, Cameron JN (1982) Respiration and acid-base physiology of the spotted gar, a bimodal breather: I. Normal values, and the response to severe hypoxia. J Exp Biol 96(1):263–280

Stevens ED, Holeton GF (1978) The partitioning of oxygen uptake from air and from water by the large obligate air-breathing teleost pirarucu (*Arapaima gigas*). Can J Zool 56(4):974–976

Val AL, Almeida-Val VMF (1995) Fishes of the Amazon and their environment. Springer-Verlag, Berlin

Val AL, Affonso EG, Souza RHS, Almeida-Val VMF, Moura MAF (1992) Inositol pentaphosphate in the erythrocytes of and Amazonian fish, the pirarucu (*Arapaima gigas*). Can J Zool 70:852–855

Verdouw H, van Echted CJA, Dekkers EMJ (1978) Ammonia determination based on indophenol formation with sodium salicylate. Water Res 12:399–402

Welker AF, Moreira DC, Campos EG, Hermes-Lima M (2013) Role of redox metabolism for adaptation of aquatic animals to drastic changes in oxygen availability. Comp Biochem Physiol A Mol Integr Physiol 165(4):384–404

Wood CM (1992) Flux measurements as indices of H^+ and metal effects on freshwater fish. Aquat Toxicol 22:239–264

Wood CM (1996) Is there a relationship between urea production and acid–base balance in fish? In: Val AL, Randall DJ (eds) Physiology and biochemistry of the fishes of the Amazon. INPA, Manaus, pp 339–357

Wood CM (2001) The influence of feeding, exercise, and temperature on nitrogen metabolism and excretion. In: Anderson PA, Wright PA (eds) Fish physiology, vol 20. Academic Press, Orlando, pp 201–238

Wood CM, Eom J (2019) The internal CO_2 threat to fish: high PCO_2 in the digestive tract. Proc Biol Sci 286(1907):20190832

Wood CM, Pelster B, Giacomin M, Sadauskas-Henrique H, Almeida-Val VM, Val AL (2016) The transition from water-breathing to air-breathing is associated with a shift in ion uptake from gills to gut: a study of two closely related erythrinid teleosts, *Hoplerythrinus unitaeniatus* and *Hoplias malabaricus*. J Comp Physiol B 186(4):431–445

Wright PA, Fyhn HJ (2001) Ontogeny of nitrogen metabolism and excretion. Fish physiology nitrogen excretion, 20th edn. Academic Press, San Diego, pp 149–200

Zall DM, Fisher D, Garner MQ (1956) Photometric determination of chloride in water. Anal Chem 28:1665–1668

Zimmer AM, Wright PA, Wood CM (2017) Ammonia and urea handling by early life stages of fish: a review. J Exp Biol 220:3843–3855

Affiliations

Bernd Pelster[1,2] · Chris M. Wood[3,4] · Susana Braz-Mota[5] · Adalberto L. Val[5]

Bernd Pelster
bernd.pelster@uibk.ac.at

Susana Braz-Mota
susanabmota@gmail.com

Adalberto L. Val
dalval@inpa.gov.br

[1] Institute of Zoology, University of Innsbruck, Innsbruck, Austria

[2] Center for Molecular Biosciences, University of Innsbruck, Innsbruck, Austria

[3] Department of Zoology, University of British Columbia, Vancouver, BC V6T 1Z4, Canada

[4] Department of Biology, McMaster University, Hamilton, ON L8S 4K1, Canada

[5] Laboratory of Ecophysiology and Molecular Evolution, Brazilian National Institute for Research of the Amazon, Manaus, Brazil